



2024

ADDITIVE AND DESIGN FOR ADDITIVE PROJECT

Gear Selector Fork Design Optimization for Additive
Manufacturing through ALTAIR INSPIRE

GROUP 8

Mahesh Muralidharan – S307783

Mudumbai Anirudh Badrinath – S309458

Arindam Balaji Rao – S310629

Ali Reza Azizi – S308541

Mohammad Bagheri – S302098

Contents

1.INTRODUCTION.....	PG
2.MATERIAL SELECTION.....	PG
3.AM TECHNOLOGY SELECTION.....	PG
4.METHODOLOGY.....	PG
5.RESULTS.....	PG
6.COSTING.....	PG
7.CONCLUSION.....	PG

1. Introduction

The gear selector fork consists of a structure with two support plates, each equipped with coaxial through-holes that facilitate the fork's sliding movement along a fixed rod within the gearbox. Additionally, the structure includes two prongs firmly attached to the body, featuring actuating portions at their ends capable of manipulating the sliding coupling sleeve of the gearbox. An actuating nose, affixed to the body, ensures the fork's sliding motion along the stationary rod, enabling the engagement of the desired gear.

The design of the body and prongs allows for the installation of two forks with identical structures on the same stationary rod, aligning partially in the direction of the sliding movement along the rod. The prongs are welded to one of the support plates on the body, extending on the same side as the welding zone concerning the axis of the through-holes.

Reducing weight in the transmission line of an automotive system can offer several advantages, impacting both the vehicle's performance and overall efficiency. A lighter transmission system contributes to a lower overall vehicle mass. This reduction in weight can result in improved acceleration and overall performance, providing a more responsive and agile driving experience. By lowering the weight in the transmission line, the engine may operate more efficiently, leading to a decrease in greenhouse gas emissions and pollutants released into the environment. Weight reduction in the transmission system contributes to a lower center of gravity and improved weight distribution. This can enhance the vehicle's handling, making it more stable and maneuverable, especially during cornering and quick directional changes. Reducing weight in the transmission line of an automotive system contributes to improved fuel efficiency, enhanced performance, and environmental benefits, making it a crucial aspect of modern vehicle design and manufacturing. In summary, reducing weight in the transmission line of an automotive system contributes to improved fuel efficiency, enhanced performance, and environmental benefits, making it a crucial aspect of modern vehicle design and manufacturing.

1.1 Main Objectives

- Weight reduction (topology optimization)
- Better Structural integrity
- Better AM Manufacturability

2. Material Selection

Choosing a material involves intricate decision-making due to the abundance of available materials and the intricate interplay of diverse properties. The mechanical aspects take precedence in component design and material selection. The process of choosing materials is implemented according to the approach outlined in "*A novel method for materials selection in mechanical design*". The first step involves identifying the essential properties based on the part's application. Once the necessary properties are pinpointed, they are prioritized in relation to each other. Subsequently, these properties are assigned weights reflecting their significance, a process known as the Weighted Properties Method (WPM).

2.1 Weighted Properties Method (WPM)

Within the framework of the Weighted Properties Method (WPM), each material property receives a specific weight (α) based on its significance. This weight factor is then applied to the scaled property of a material, resulting in a weighted property value. By summing up the weightages, performance values (γ) are derived. This process is repeated for every potential material. The material deemed most appropriate is the one with the highest performance value. The weightage of properties is determined as shown in Table below. Each property is compared with every other property. When comparing two properties, the most significant property is assigned with a value of three(3), and the least significant is given with a value of one(1). If the properties are equally important, both are given a value of two(2). The relative weighting factor (α) is obtained by dividing significant decisions for a property by the total significant decisions of all properties. Now each property of probable materials is scaled such that the highest value does not exceed a hundred. For a given property, the scaled value (X) of that property comparing all the materials is equal to

$$X = \frac{\text{numerical value of the property}}{\text{maximum value in the list}} \cdot 100 \quad (\text{x.x})$$

Table 2.1: Comparing Required Properties to Determine Relative Weightage

Properties	<u>Significance of the Properties</u>										Significant Decisions	Weightage (α)
	1	2	3	4	5	6	7	8	9	10		
A	3	3	3	1							10	0.250
B	1				1	1	1				4	0.100
C		1			3			2	1		7	0.175
D			1			3		2		1	7	0.175
E				3			3		3	3	12	0.300

The performance index is computed by multiplying each weighted property with the corresponding scaled property of the material and subsequently summing all the properties to obtain a performance value.

$$\gamma = \sum_{i=1}^n (X_i)(\alpha_i) \quad (x.y)$$

The main alloying elements in the low alloy steels and their properties contributed to the alloy are as follows:

Table 2.2: Alloying elements and properties contributed to alloy

Elements	Properties
Cr	Anti Corrosion, hardest material
Ni	Heat Resistant, high hardness, scratch resistant
Cu	Corrosion resistant, austenitic microstructure
Mo	High heat resistant, excellent conductor
Mn	Hardness and strength
V	Wear Resistant
Si	Deoxidizer
C	Hardening Agent
S	Impurity, reduces weldability
P	Impurity

Table 2.3: Chemical composition of probable materials in weight percentage.

Element Alloys	Carbon	Manganese	Chromium	Molybdenum	Silicon	Phosphorus	Sulfur
AISI 4142	0.40-0.45	0.75-1.0	0.8-1.1	0.15-0.25	0.15-0.35	Negligible	Negligible
AISI 4130	0.28-0.33	0.40-0.60	Negligible	0.15-0.25	0.15-0.35	0.04	0.04

The availability of the material is also a very important aspect. Hence, the choice of steel was an obvious one. The abundance of availability, cost effective nature, easily manufacturable in the required shape and the load withstanding capability all contribute to this choice.

3. AM Technology Selection

The prevalent metal AM technologies are powder bed fusion (PBF) and directed energy deposition (DED).

Since we do not want high volume production rate and our structure is not large, we chose PBF.

Listed here are some advantageous of PBF that make it suitable over DED for fork gear selector:

Precision and Detail

PBF processes, especially SLM, are known for their high precision and ability to produce intricate details. This can be advantageous for applications that require fine features and complex geometries.

Material Properties

PBF processes can provide excellent material properties, such as high density and good mechanical performance. This is critical for applications where the strength and integrity of the final part are paramount

Surface Finish

Generally, PBF offers superior surface finish compared to DED.

4-Post-Processing

Typically, PBF requires less post-processing

Machine Availability and Cost

Consider the availability of machines for each process and the associated costs. PBF machines are more common.

For a fork gear selector, which may require precision and detail, PBF could be a suitable choice. Between SLM and DMLS, the **SLM** is chosen because it is more commonly used for metal alloys due to its ability to achieve full density, therefore improved mechanical properties. Also, it has better surface finish and the residual stresses are reduced in which is crucial for components like selector forks, where dimensional accuracy and stability are essential for proper functionality.

4. Methodology

The step file of the gear selector fork is loaded into Inspire 2022. The workflow we have decided with the project is to first choose a suitable material for the part. As discussed earlier the preferable material chosen for the model is AISI 4142 but we are also running the optimisation using AISI 4130. The model is 58 mm * 74mm *16 dimensionally.

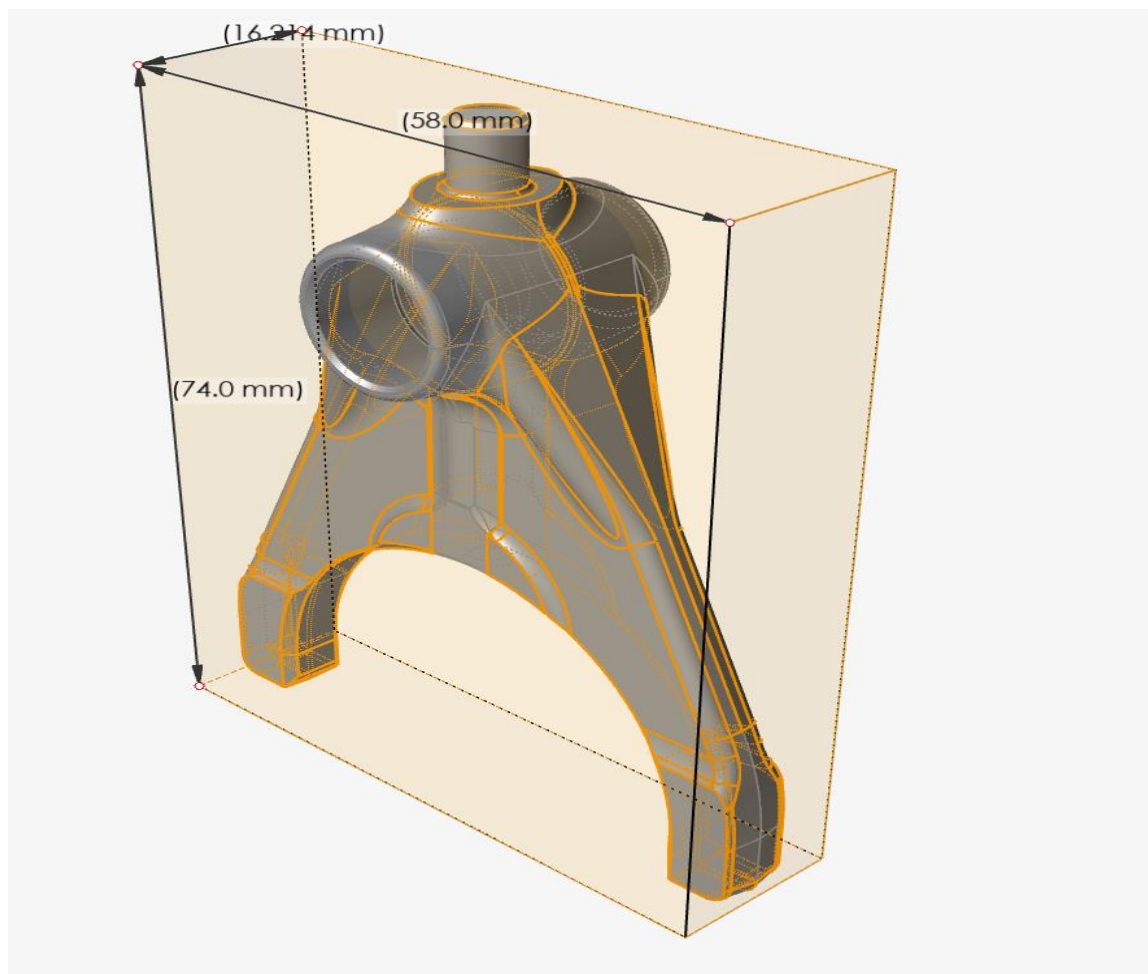


Figure 3.1 – Dimensions of the model

We first use the property editor in inspire to assign the material STEEL – 4142 to the model (we will assign AISI 4130 and redo the steps from optimisation onwards for comparison of materials). Now we need to separate our model into design space and non- design space so that inspire knows which parts of the

model to optimize and which parts to not, lest the integrity or the function of the part be affected. In our model the transmission shaft seat which is connected to the lubrication pathway and the main selector fork contact points with the gears that is the gear selector fork legs are chosen as non-design spaces as they are integral to the function of the part. The separation of design and non - design space is done using the partition tool.



Figure 3.2 – Design and non-design space.

4.1 Loads

We now move to applying a load to the model. The loads were applied to the points 1 and 2 shown in the figure below which are the legs of the gear selector fork and the main interacting contact surface the selector fork has with the gear sleeves within the vehicle transmission. The reaction forces from the gears to the gear selector fork will thus be applied to these points and as such the loads are applied there.

A Total load of 600N is applied.

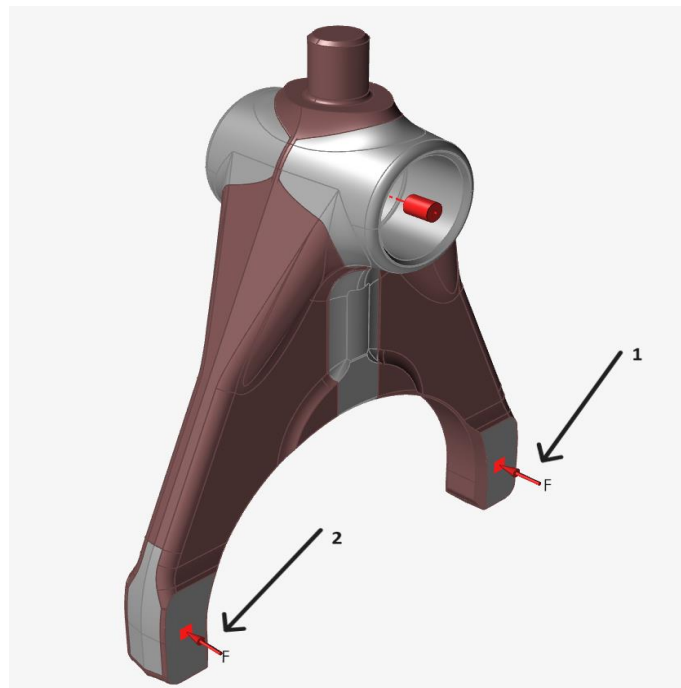


Figure 3.3 – Load points

4.2 Constraints

We have to apply some constraints to the model before we move on to topology optimization.

The first of the constraints we have to apply is a DoF restriction in the form of the support tool. We use the support tool to apply the constraint to the transmission shaft seat. As shown in figure 3.3

In inspire, often while performing topology optimisation there is an irregular material removal across the part which in the case of most parts would compromise structural dependencies. In the case of our model an uneven optimisation would result in an unbalanced mass distribution which would lead to sub optimal reaction to loads applied on the critical areas and would create complications during gear shifts and thus affect overall transmission quality which would lead to consequences in ergonomics. To prevent this, we apply a constraint in the form of the shape control tool and create symmetry planes using the symmetric controls sub tool so that when inspire is performing the topology optimisation it will perform the optimisation evenly so that mass distribution isn't irregular

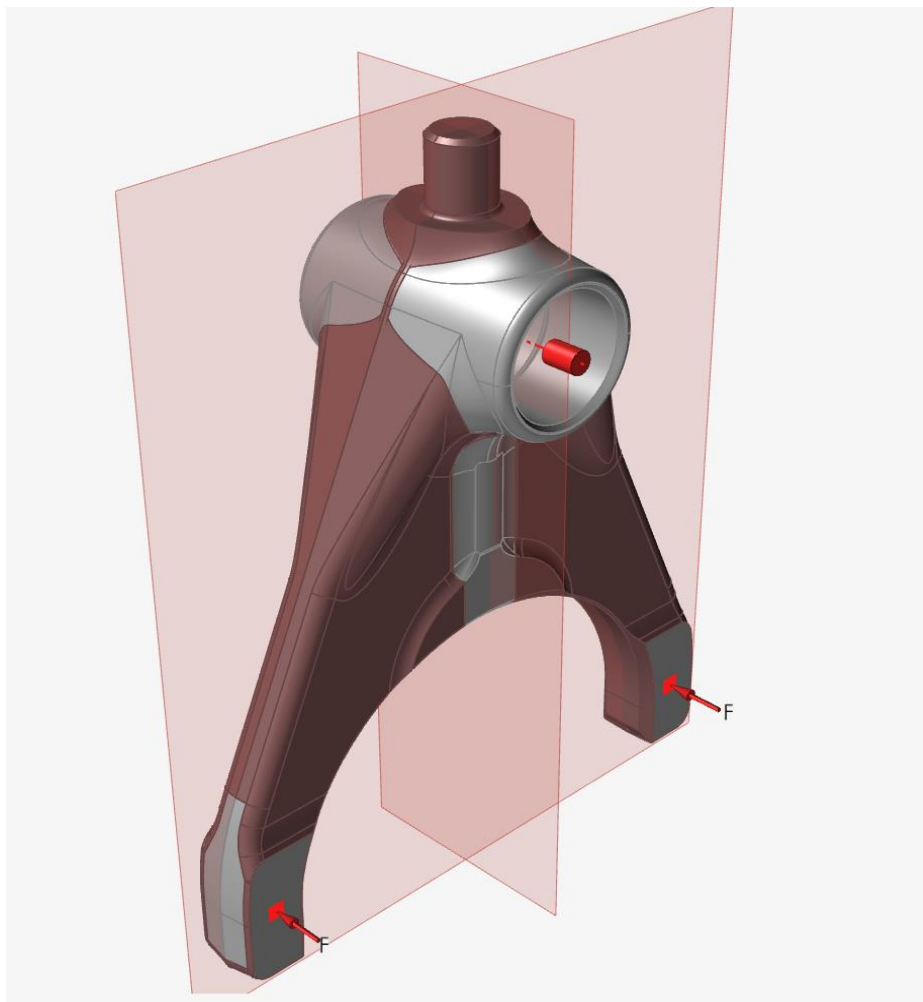


Figure 3.4 – Symmetry planes.

4.3 Optimisation

With all the constraints and loads applied, it is now time to perform the topology optimisation. The workflow we have chosen here is to first perform an optimisation with the objective set to minimize mass and then performing an optimisation with the objective set to maximize stiffness after retrieving the mass of the model obtained from the minimize mass iteration. The rationale for this workflow is that the minimize mass objective returns a model with a reduced mass while being able to support the loads applied while respecting a safety factor constraint that we have chosen. The base model has a safety factor of 3.2 so we apply a safety factor of 2 as a constraint during the minimize mass topology optimisation. Applying a higher safety factor would result in a higher mass retention while a lower safety factor as a constraint would be objectionable from a transmission component safety point of view.

After the new geometry is obtained, we proceed to analyse it using the run optistruct analysis tool. After this we retrieve the total mass of the optimised model so that it can be used as the targeted mass during the maximise stiffness topological optimisation objective run. Continuing from the earlier explanation of rationale this is done so as while the minimise mass objective returns the minimum mass of the part which is able to support the load maximize stiffness can return an optimised part for the same mass with better stress tolerance capability.

We analyse this new part.

4.4 Problems encountered during design refinement

Normally after an optimised part is obtained, we would then use either POLYNURBS FIT or most commonly POLYNURBS WRAP to create a new POLYNURB part so as to obtain a smooth, sharp and clean design. In the case of our optimisation runs the parts obtained were comparatively sharper and clean but still had lots of minor imperfections. We tried to use POLYNURBs wrap but the tool wasn't able to capture the optimised part geometry. We then sought to use fit which while being able to capture the geometry missed out on a lot of the part details. The default POLYNURBs faces is set to 2500. Reducing it will cause the POLYNURBs fit to miss out a lot of part details while increasing it will increase the part complexity while not returning part detail satisfyingly.

5. RESULTS

5.1 Survey of results

The final model was obtained it by two iterations of topology optimization, i.e., using minimize mass and maximize stiffness. We use two types of material to compare and determine which is the better one to use. The materials used are Steel (AISI 4142) and Steel (AISI 4130).

5.1.1 Steel AISI 4142

First Iteration (Minimize mass)

The mass of our iteration is 51.191g.

We applied a force of 600N obtained the following results:

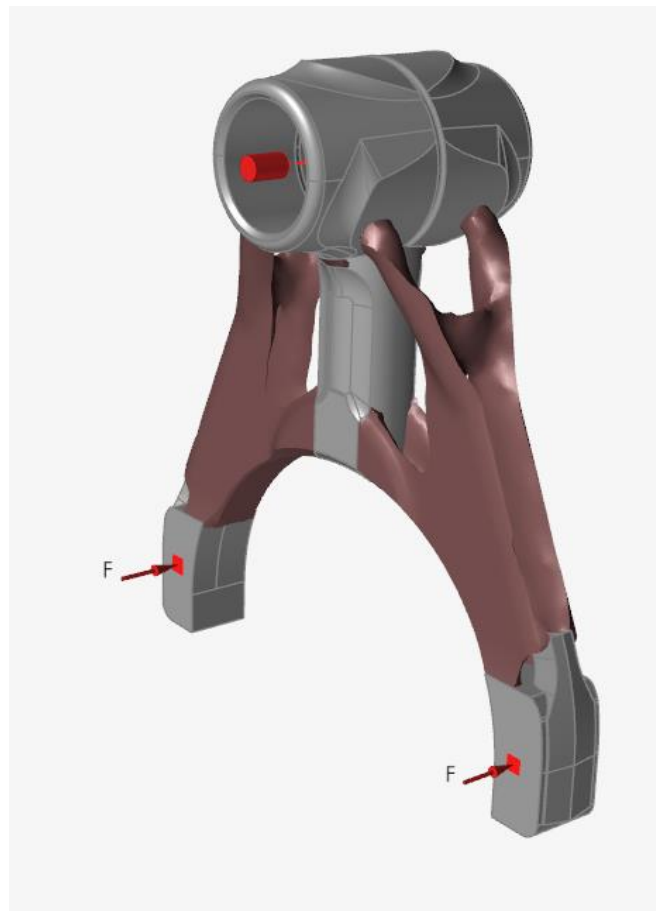


Figure 5.1 - Isometric View

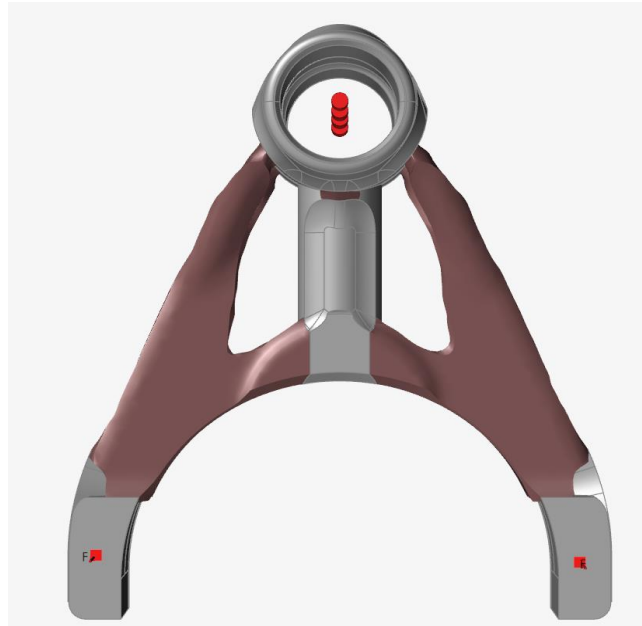


Figure 5.2 - Front View

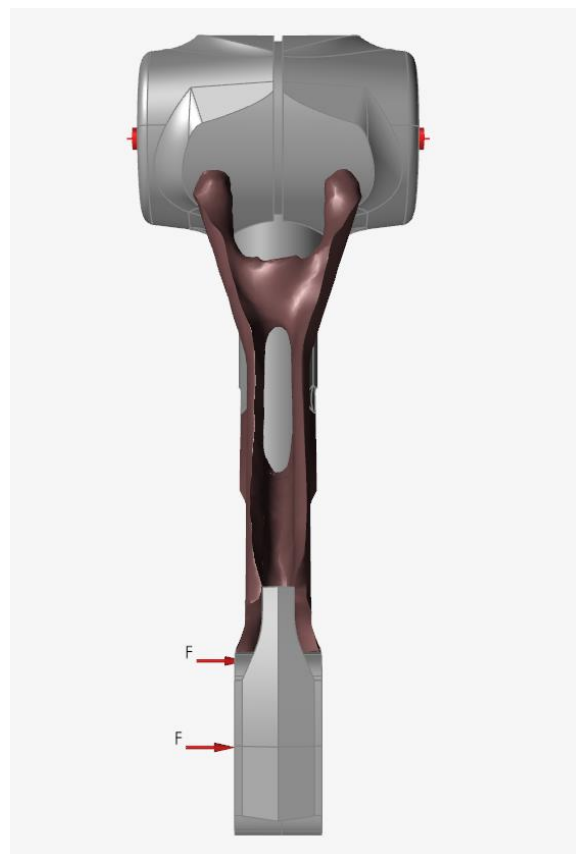


Figure 5.3 - Side View

We obtain our FEM analysis results concerning the displacement, von Mises stress and the Factor of safety.

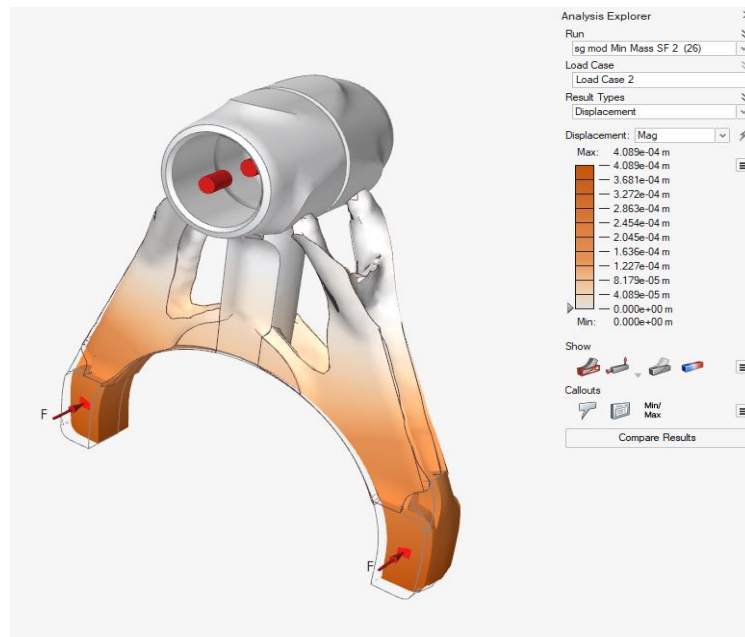


Figure 5.4 - Displacement Isometric View

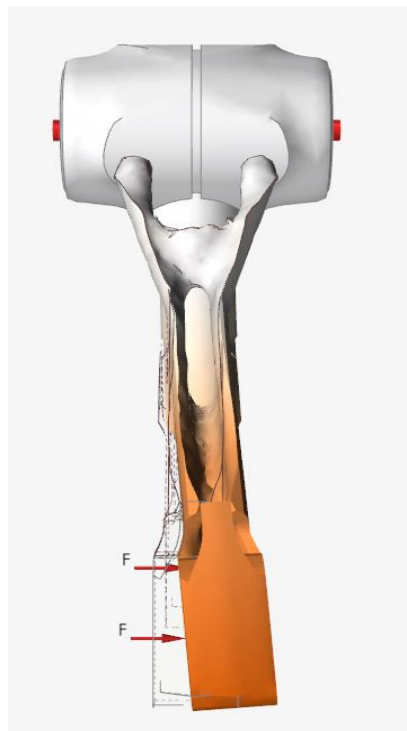


Figure 5.5 - Displacement Side View

From the above figures the displacement is clear and we got a value of **0.4089 mm**.

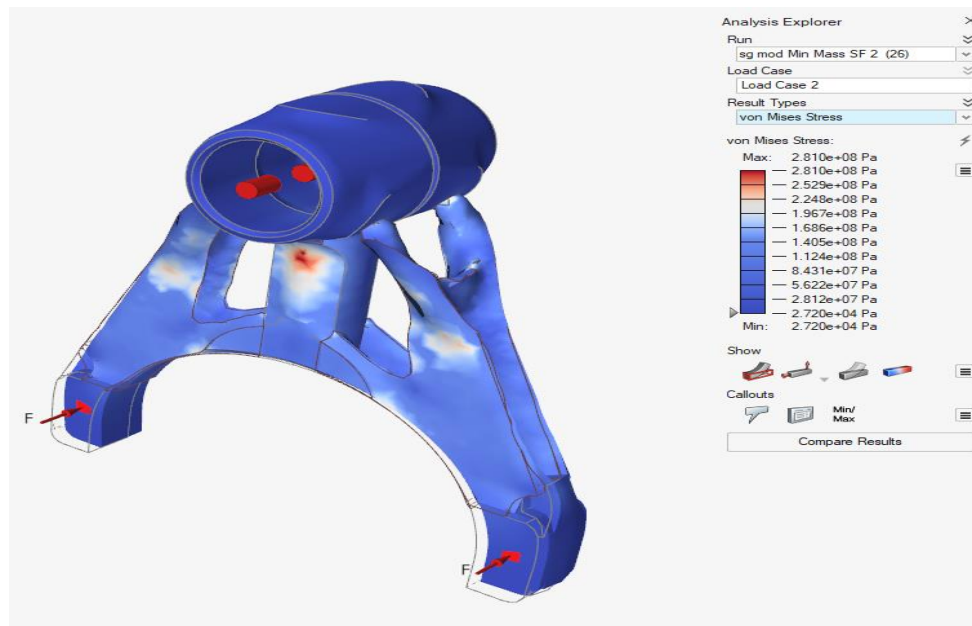


Figure 5.6 - von Mises stress isometric view

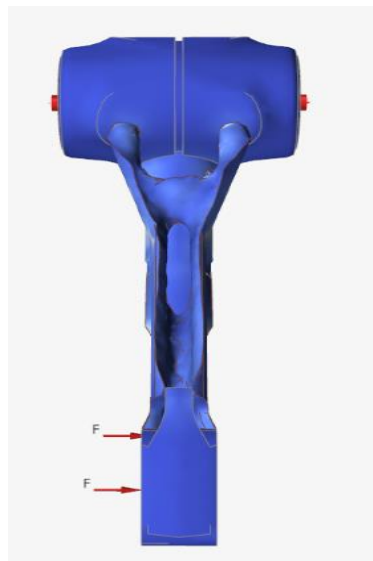


Figure 5.7 - von Mises stress side view



Figure 5.8 - von Mises stress front view

From the above figures the maximum von Mises stress value we obtained was **281 MPa**.

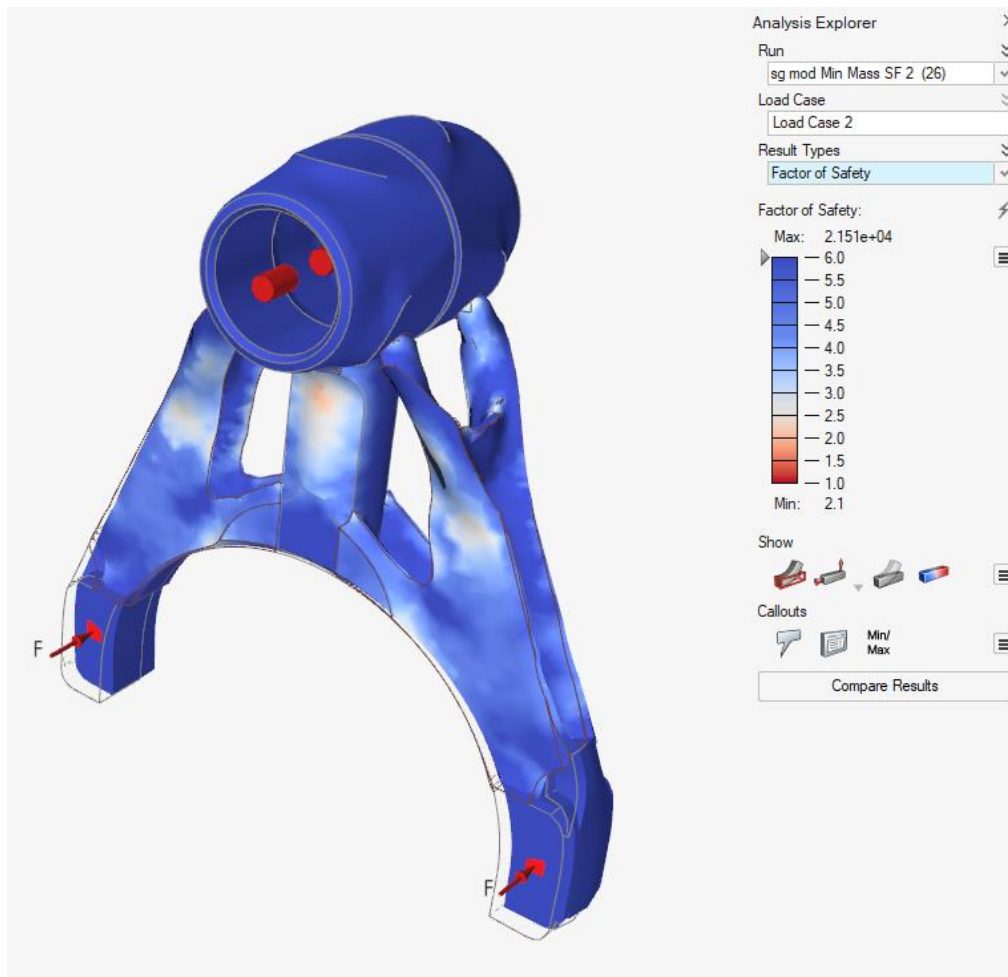


Figure 5.9 - Factor of Safety

From the above figure the minimum Factor of Safety as **2.1**.

Furthermore, we have a mass reduction of at least **39.5%** while maintaining the desired Factor of Safety.

Second Iteration (Maximize Stiffness)

The mass of our iteration is 52.184 g.

We applied a force of 600N and obtained the following results:

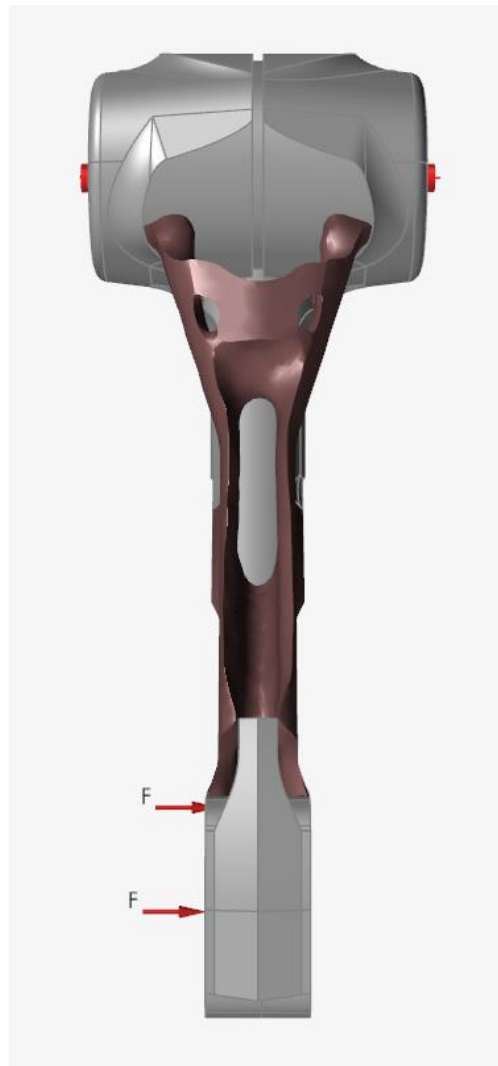


Figure 5.10 - Side View



Figure 5.11 - Isometric View



Figure 5.12 - Front View

We obtain our FEM analysis results concerning the displacement, von Mises stress and the Factor of safety.

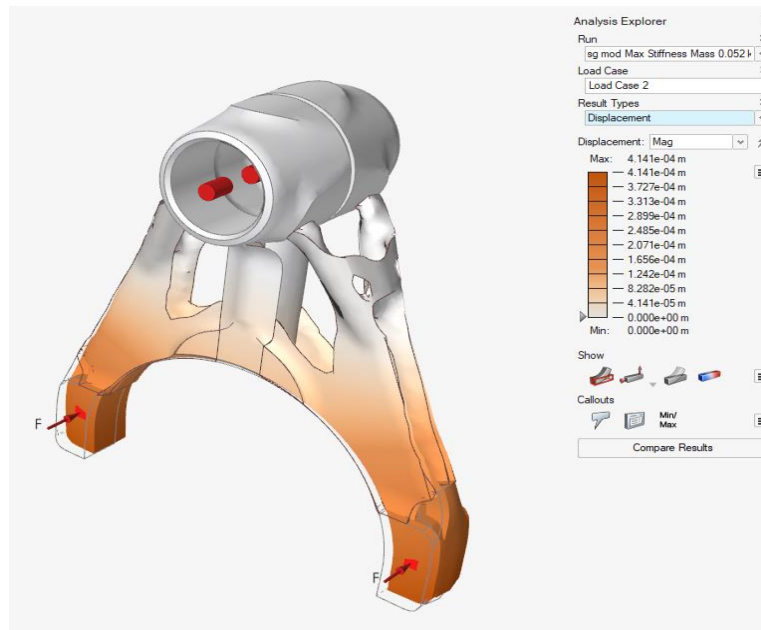


Figure 5.13 - Displacement Isometric View

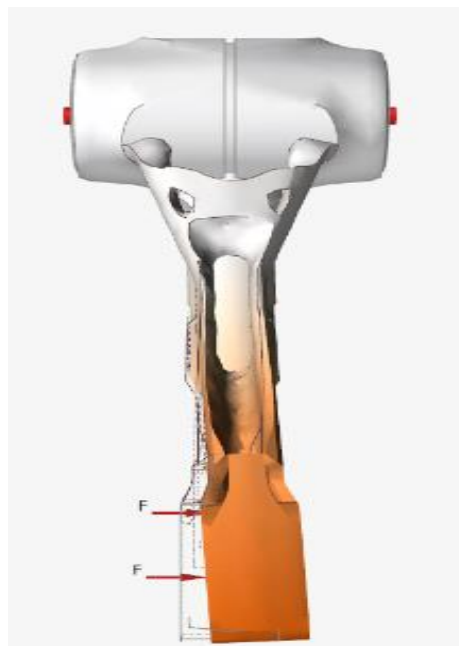


Figure 5.14 - Displacement Side View

From the above figures the displacement is clear and we got a value of **0.4141 mm**.

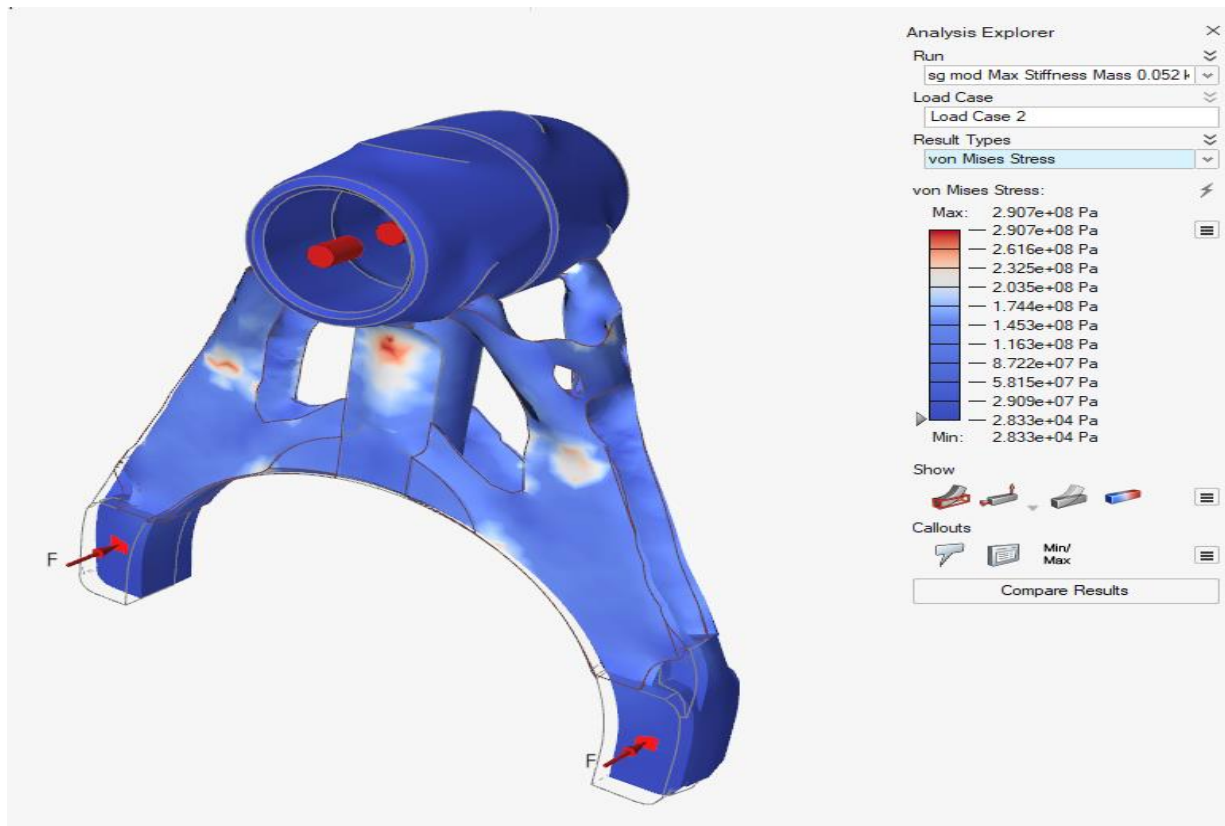


Figure 5.15 - von Mises stress Isometric view



Figure 5.16 - von Mises stress side view



Figure 5.17 - von Mises stress front view

From the above figures the maximum von Mises stress value we obtained was **290.7 MPa**.

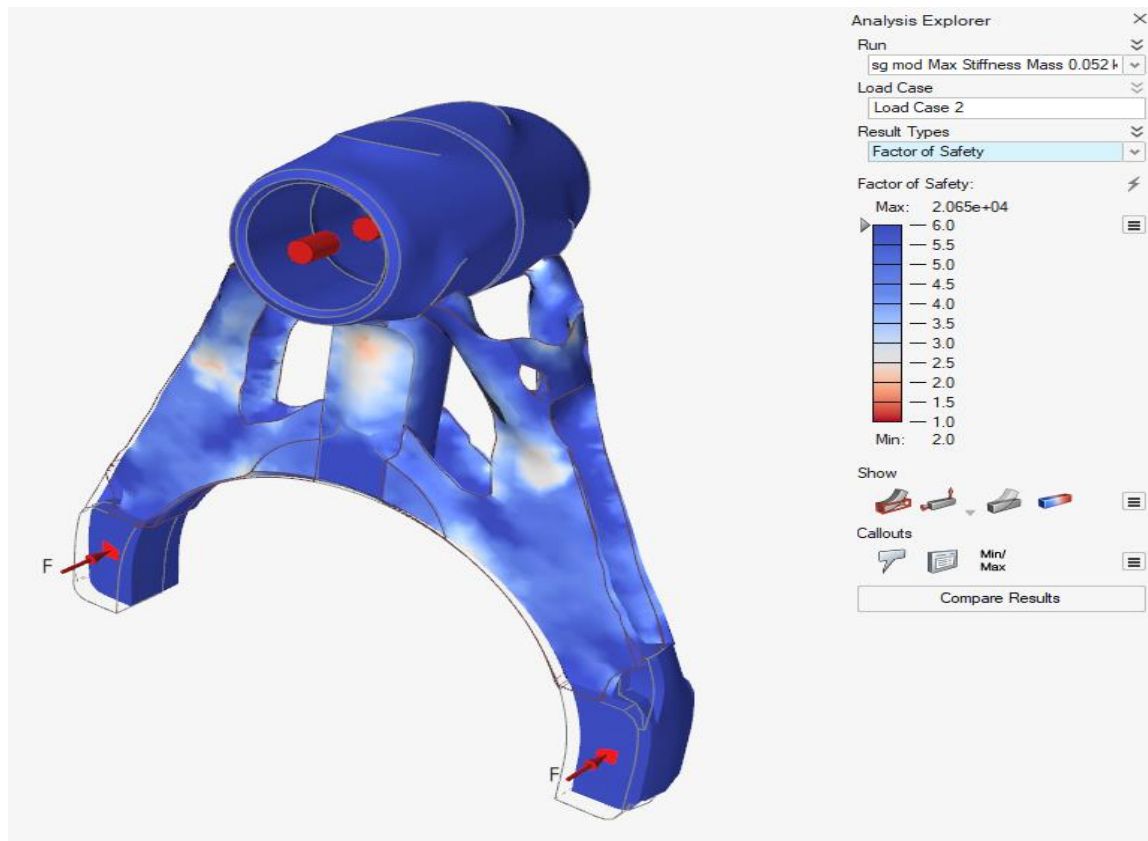


Figure 5.18 - Factor of Safety

From the above figure the minimum Factor of Safety as **2.0**.

5.1.2 Steel AISI 4130

First Iteration (Minimize mass)

The mass of our iteration is 51.191g.

We applied a force of 600N obtained the following results:



Figure 5.19 - Isometric View

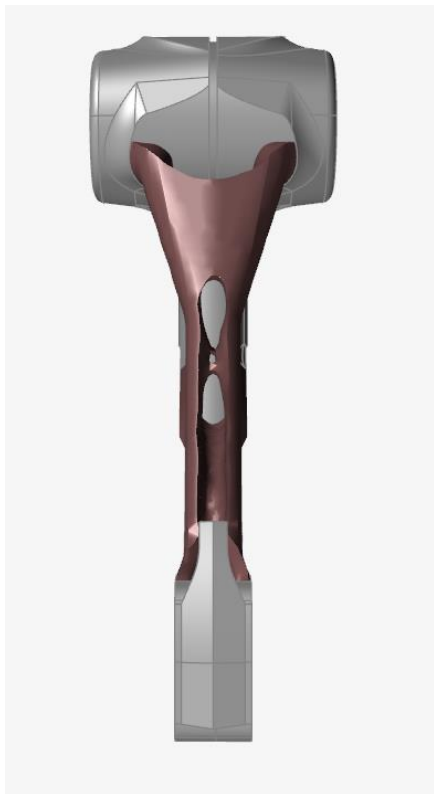


Figure 5.20 - Side View



Figure 5.21 - Front View

We obtain our FEM analysis results concerning the displacement, von Mises stress and the Factor of safety.

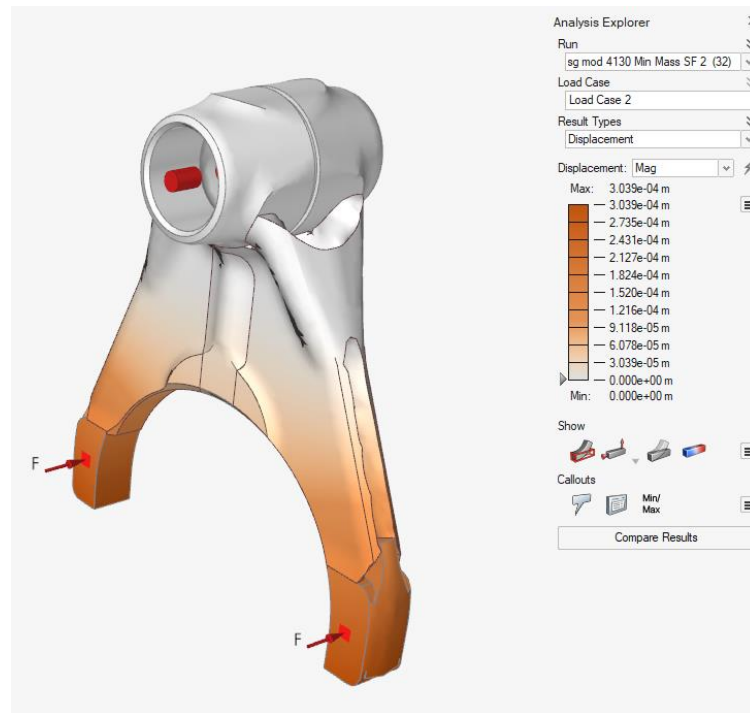


Figure 5.22 - Displacement

From the above figure the displacement is clear and we got a value of **0.3039 mm**.

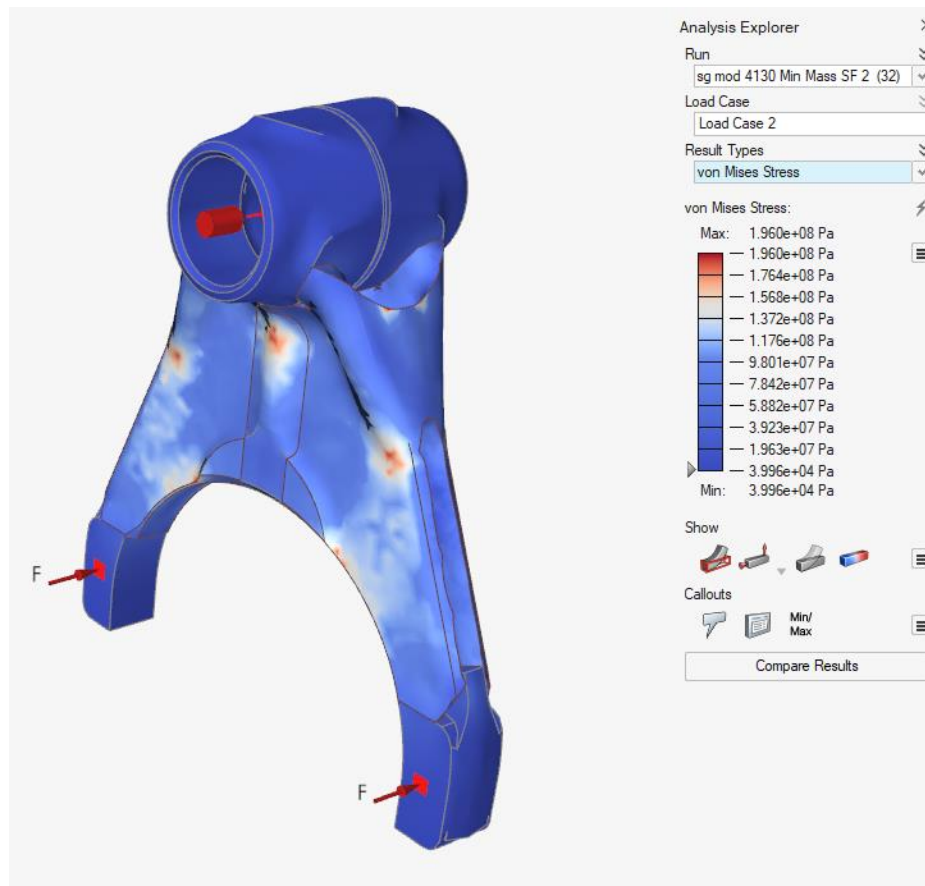


Figure 5.23 - von Mises stress

From the above figures the maximum von Mises stress value we obtained was **196 MPa**.

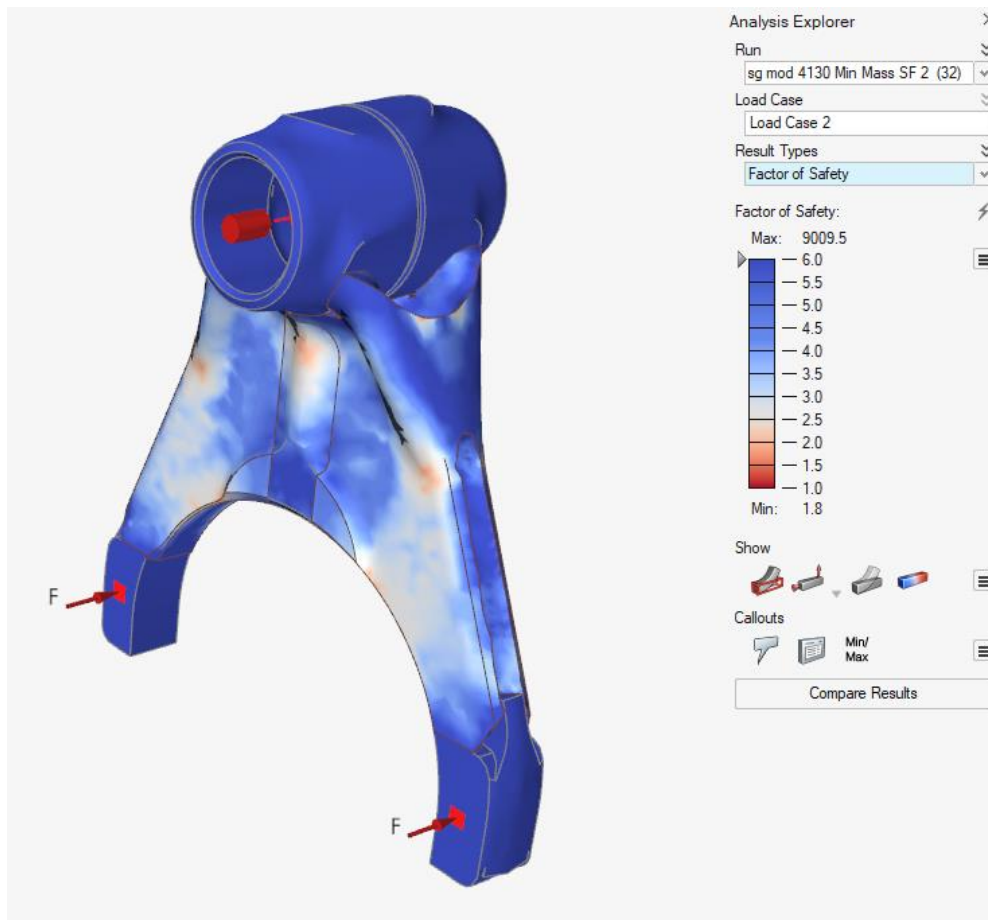


Figure 5.24 - Factor of Safety

From the above figure the minimum Factor of Safety as **1.8**.

Second Iteration (Maximize Stiffness)

The mass of our iteration is 52.184 g.

We applied a force of 600N and obtained effectively the same structure as the second iteration of Steel AISI 4142.

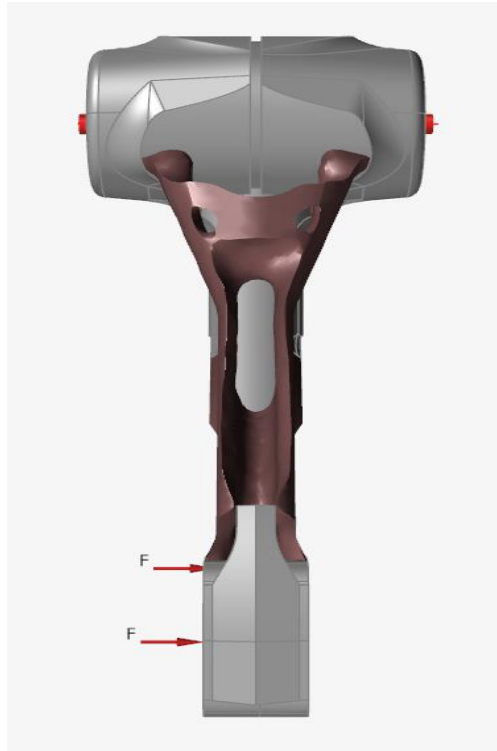


Figure 5.25 - Side view

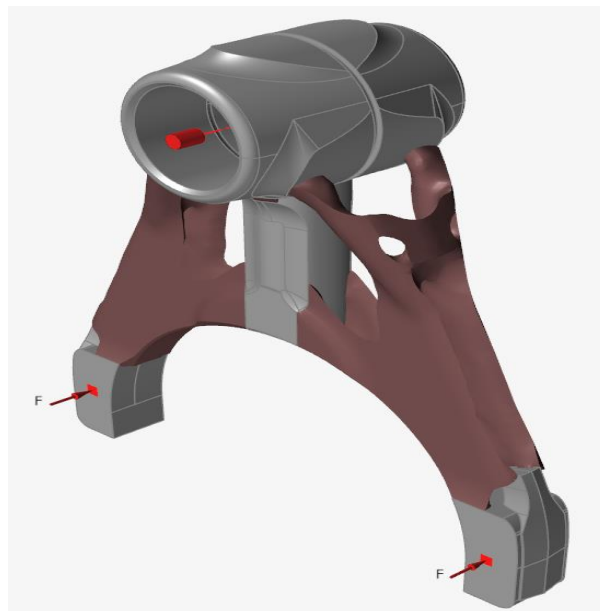


Figure 5.26 - Isometric view



Figure 5.27 - Front view

We obtain our FEM analysis results concerning the displacement, von Mises stress and the Factor of safety.

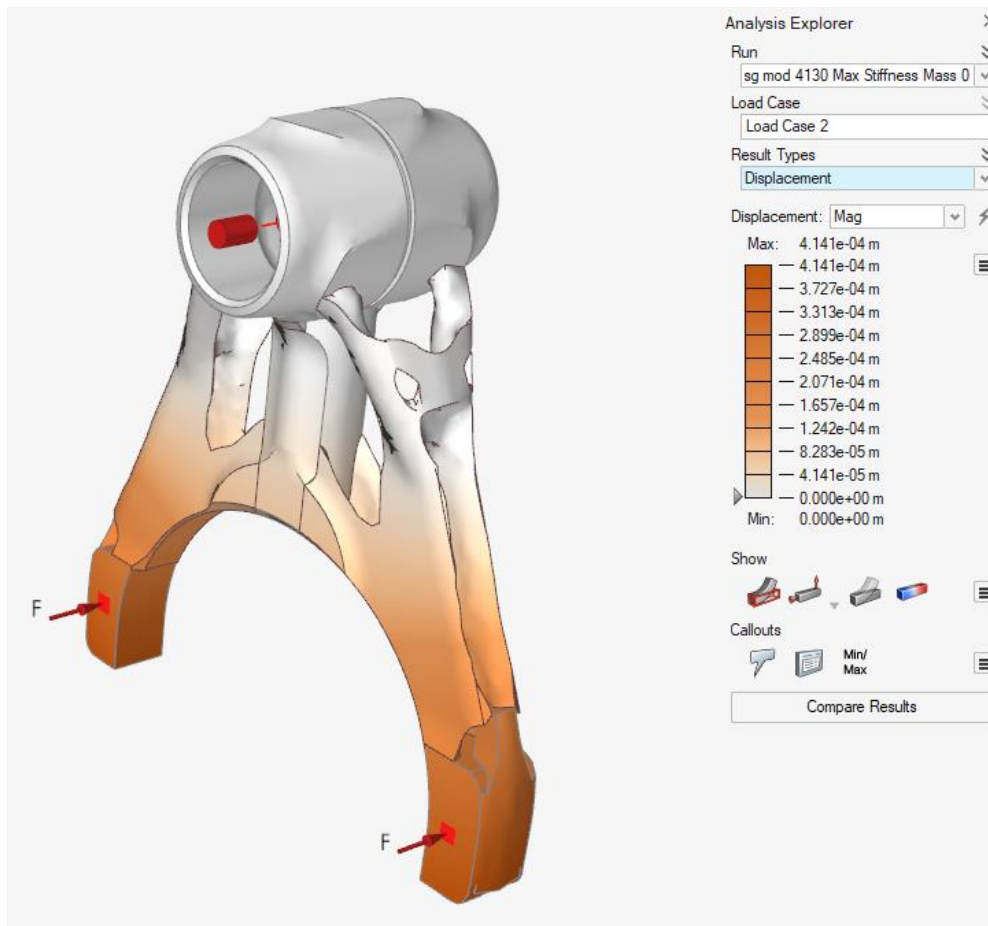


Figure 5.28 - Displacement

From the above figure the displacement is clear and we got a value of **0.4141 mm** which is the same as the displacement as the second iteration of Steel AISI 4142.

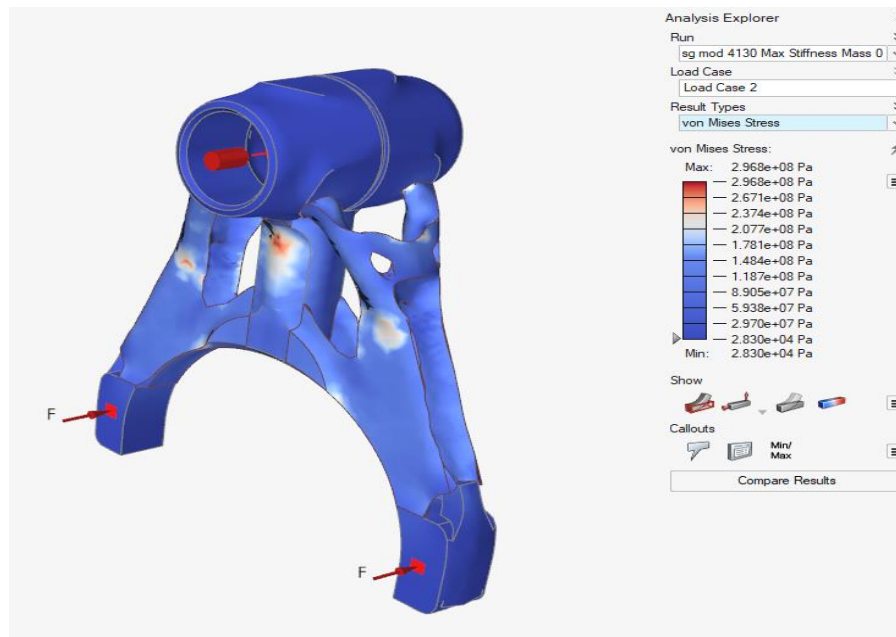


Figure 5.29 - von Mises stress

From the above figures the maximum von Mises stress value we obtained was **296.8 MPa**.

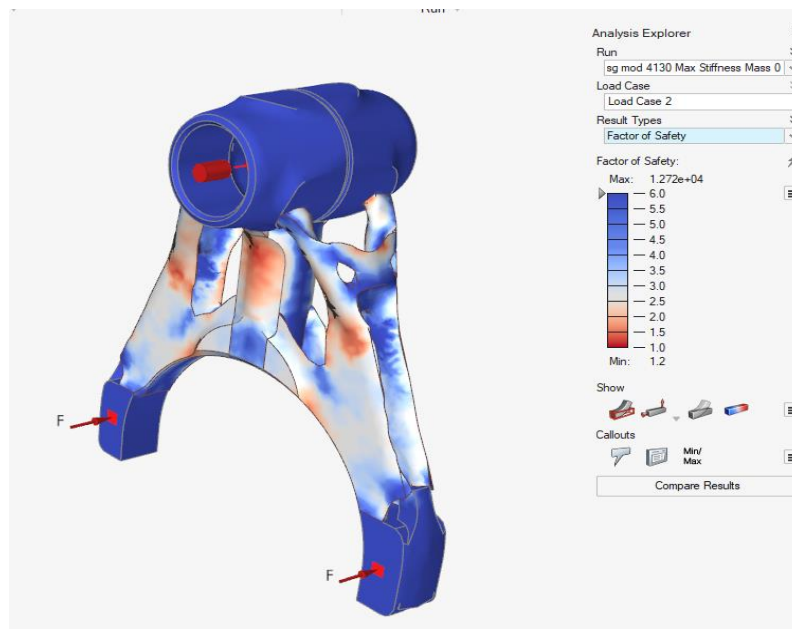


Figure 5.30 - Factor of Safety

From the above figure the minimum Factor of Safety as **1.2**.

5.2 Analysis of Results

The analysis provides us with a major difference between the base model and the two iterations. It also highlights the difference in the two materials used and gives us an idea of which material is better in this application.

While comparing the base model and the first iteration it is observed that the first iteration, i.e., minimize mass, is naturally subject to lower stress. The key point being the Factor of Safety which determines the amount of mass minimized during optimization.

We then use that mass value to analyze the second iteration. When we compare the first and second iteration we observe that the second iteration, physically, has more material on the sides than the first iteration and this effectively contributes to the higher stress resistance with a lower safety factor.

When we compare both the material we can observe that AISI 4142 has a higher stress resistance than AISI 4130. Though the second iteration for both materials is structurally the same AISI 4130 has a lower Factor of Safety which is not optimal for our design.

6. Costing

6.1 Conventional process

Conventional process for manufacturing a gear selector fork involves forging, heat treatment, machining, surface treatment, inspection. Concerning labour costs, we evaluated:

- Forging: €30
- Heat treatment: €20
- Machining: €25
- Surface treatment: €20
- Inspection: €10

Average prices for the machinery used in each step of the manufacturing process required, involves:

Raw Material Preparation

- Bar cutting machine: €40,000

- Annealing furnace: €20,000

Forging

- Hammer press: €75,000
- Drop forging machine: €20,000
- Roll forging machine: €250,000

Heat Treatment

- Quenching tank: €7,000
- Tempering furnace: €15,000

Machining

- Lathe: €10,000
- Milling machine: €10,000
- Drilling machine: €15,000
- Grinder: €10,000

Surface Treatment

- Nitriding furnace: €15,000
- Carburizing furnace: €20,000
- Painting booth: €20,000

Inspection

- Callipers: €400
- Micrometres: €800
- Optical comparators: €4,000

Cost evaluation considerations in traditional method:

It is notable that hourly cost of machine has been calculated utilizing the following procedure:

- Purchase cost of forging equipment
- Depreciation rate: 25%
- Annual depreciation
- Machine maintenance costs per year: 10% of the initial price
- Average electricity consumption of the the equipment
- Electricity cost per kWh: € 0.30

Hourly machine cost = Hourly depreciation + Hourly electricity cost + hourly machine maintenance cost.

The mass of each product has been considered including 30% waste through manufacturing process.

Lot size	(pcs)	10
Material cost per kg	(€/kg)	33
Part weight	(kg)	0.07
Material cost	(€)	2.31
Forging time needed	(h)	1.5
Set-up time	(h)	0.1
Non-productive time	(h)	0.5
Hourly cost of machine	(€/h)	30.31583
labour cost	(€/h)	30
Forging cost	(€)	126.6632
Part program generation	(€)	20
Machining time needed	(h)	4
Set-up time	(h)	0.1
Non-productive time	(h)	0.5
Hourly cost of machine	(€/h)	7.997717
labour cost	(€/h)	30
Machining cost	(€)	194.7895
Heat treatment time needed	(h)	6
Set-up time	(h)	0.1
Non-productive time	(h)	0.5
Hourly cost of heat treatment*	(€/h)	60.97666
labour cost	(€/h)	25
Heat treatment cost	(€)	99.08708
Surface treatment time needed	(h)	1
Set-up time	(h)	0.1
Non-productive time	(h)	0.25
Hourly cost of machines	(€/h)	50
labour cost	(€/h)	20
Surface treatment cost	(€)	62.5
Inspection time needed	(h)	1
Hourly cost of machines	(€/h)	2.930847
labour cost	(€/h)	10
Inspection cost	(€)	12.93085
Building cost	(€)	483.0398
TOTAL COST PER STRUCTURE	(€)	485.3498
production rate	(pcs/h)	0.31746

Table 6.1 – Costing table for conventional method

Examining the production volume of 10 products, the allocated costs for each can be compared through the chart presented below:

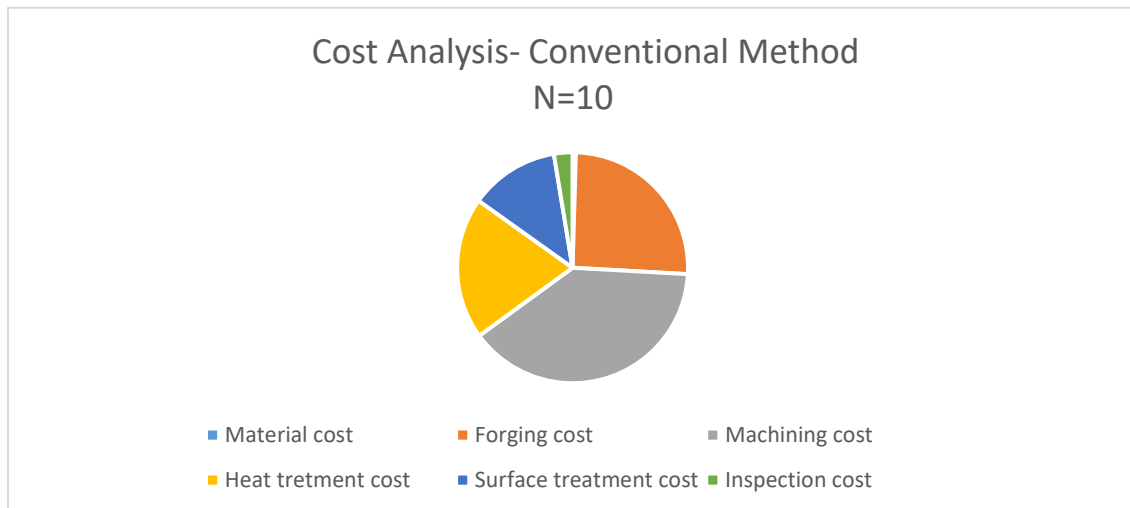


Figure 6.1 – Cost split conventional

6.2 SLM process cost analysis

In the evaluation of our chosen Additive Manufacturing (AM) machine, namely the EOS M290, a comprehensive analysis was performed, considering specifications including build volume, power consumption, and other factors. This detailed assessment aimed to provide a comprehensive understanding of the machine's performance characteristics and operational requirements. Subsequently, the associated costs were examined to assess the economic implications of utilizing the EOS M290 for our production needs. The findings contribute into the economic feasibility and efficiency of this AM technology into our manufacturing processes.

Considerations in cost evaluation in AM process:

The hourly cost of the machine has been computed using a similar methodology as employed in the conventional method.

Mass calculations include an additional 20% for support material and waste.

Lot size	(pcs)	10
Redesign cost	(€/pcs)	50
Material cost per kg	(€/kg)	150
Part weight, including supports	(kg)	0.1
Material cost	(€)	15
Machine price	(€)	700000
Operational hours per year	(h)	7884
Service life	(years)	7
Maintenance cost per hour	(€/h)	8.878742
Power consumption	(kW)	16.7
Electricity price	(€/kWh)	0.3
Machine cost per hour	(€/h)	36.0856
Build time	(h)	50
Machine cost per build	(€)	1804.28
Machine operator cost per hour	(€/h)	30
Set-up, warm-up, cool-down of machine	(h)	1.5
Parts per build	(-)	14
Building cost	(€)	132.0914
Machine operator cost per hour	(€/h)	35
Post-processing time per build	(h)	10
Heat treatment cost per build	(€)	30
Post-processing machining cost	(€)	27.14286
TOTAL COST PER STRUCTURE	(€)	224.2343
Production rate	(pcs/h)	0.271845

Table 6.2 – SLM costing

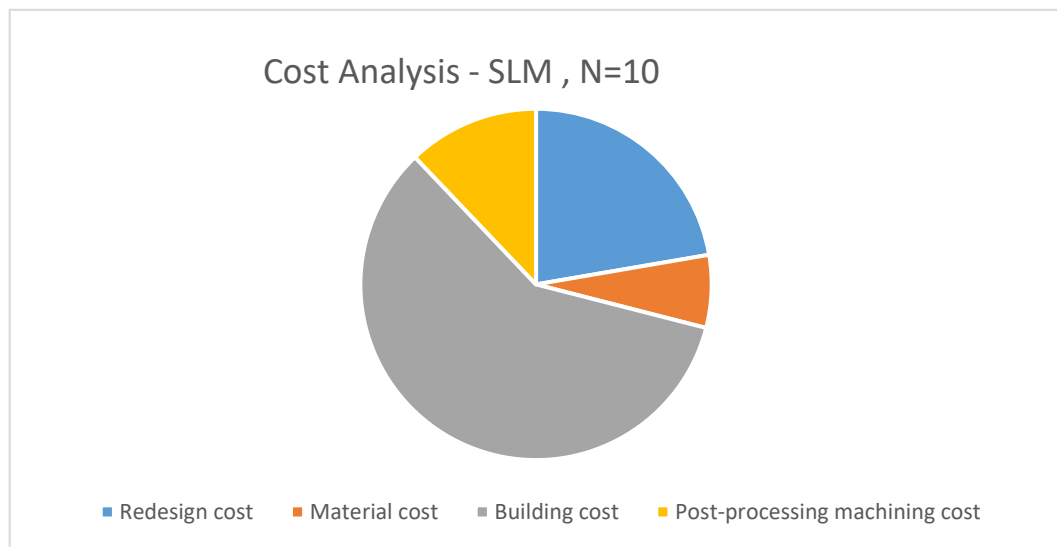


Figure 6.2 – Cost Split SLM

6.3 Break-even Analysis

To assess the economic perspective, a break-even analysis has been conducted.

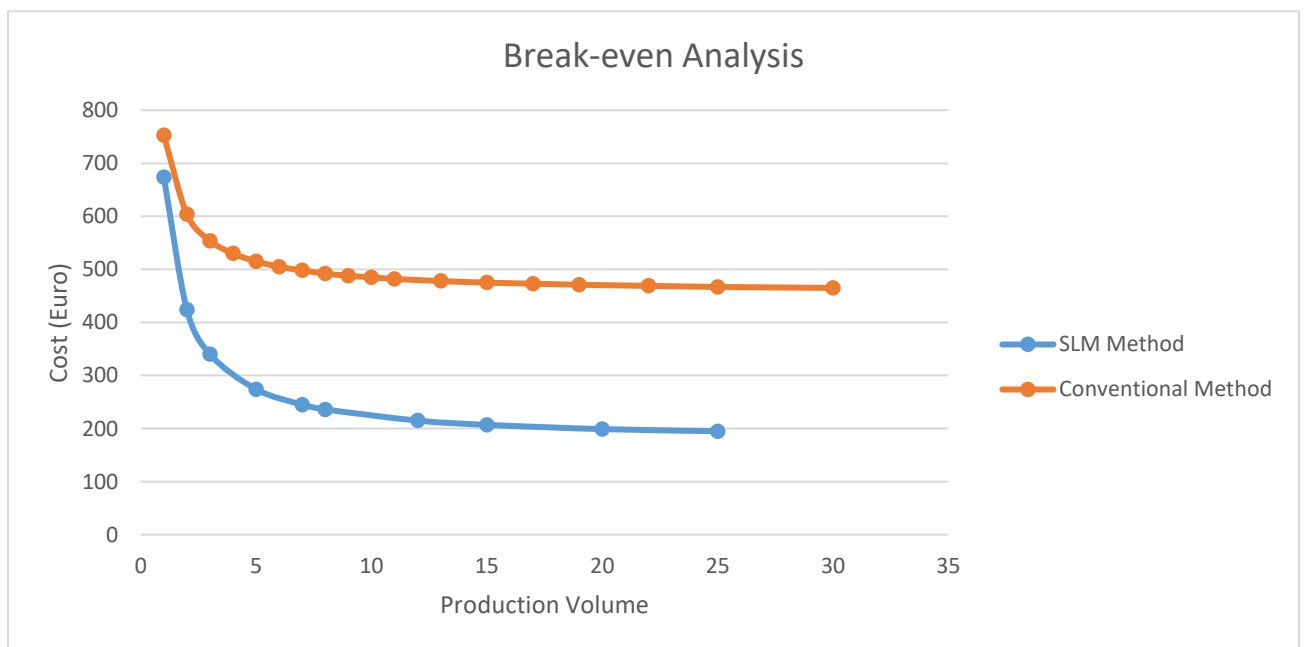


Figure 6.3 – Break Even Analysis

6.4 Discussion on the results

Costs comparison

As evident from the results, there are no intersections between the cost curves of the Selective Laser Melting (SLM) method and the Conventional Method. Additionally, the Additive Manufacturing (AM) method consistently proves to be more economical compared to the traditionally employed method at a similar production volume.

Production rate comparison

When analysing the manufacturing time for each product, it is evident that the production rate in the Selective Laser Melting (SLM) process consistently lags behind that of the traditional method. From this perspective, the traditional method demonstrates better efficiency in terms of production speed.

References

Sources for labour costs:

- ISTAT: <https://www.istat.it/>
- Confartigianato: <https://www.confartigianato.it/>
- Confindustria: <https://www.confindustria.it/>

Sources for machinery prices for the manufacturing process:

- Machinery World: <https://www.machineryworld.com/>
- Metalworking Network: <https://www.win-metalworking.com/>
- ThomasNet: <https://www.thomasnet.com/>
- MachiningMarket: <https://www.precedenceresearch.com/machining-market>
- IMTA: <http://imta.it/>

Sources for material:

- <https://www.eurofer.com/en/>

Sources for AM process:

- Hopkinson, Neil, and Phill M. Dickens. "Analysis of Rapid Manufacturing – Using Layer Manufacturing Processes for Production." Proceedings of the Institution of Mechanical Engineers, Part C : Journal of Mechanical Engineering Science. 2003. 217(C1): 31-39.
- "The Economic Impact of In-situ Monitoring Tools in Metal Additive Manufacturing (AM)" by B. M. Colosimo, S. Cavalli, and M. Grasso.

7. Conclusion

The gear selector fork is a component subject to various loads in rapid succession so it is important to determine a good material so resist the high stresses and strains. From the above analysis we have observed that the structure is ultimately dependent on the material used. We have compared two types of steel, i.e., AISI 4142 and AISI 4130 and found that the latter has a better resistance to high stress at lower Factor of Safety.

The reduction of mass of around 39.5% between the two iterations plays an important role in the components application as it is effectively lighter and more stress resistant. The use of Additive Manufacturing processes also is a way to save material and efficient production without compromising the properties of the component.

The result is that Steel AISI 4142 is the better material for this application and Steel AISI 4130 can be used as an alternative despite its clear structural weakness.